

| 発表者氏名 | 論文タイトル名 | 発表誌名 | 巻号 | ページ | 出版年 |
|--|--|------------------------------|---------|-----------|------|
| Aoyama H, <u>Shirato H</u> , Tago M, Nakagawa K, Toyoda T, Hatano K, Kenjo M, Oya N, Hirota S, Shioura H, Kunieda E, Inomata T, Hayakawa K, Katoh N, Kobashi G. | Stereotactic radiosurgery plus whole-brain radiation therapy vs stereotactic radiosurgery alone for treatment of brain metastases: a randomized controlled trial. | JAMA | 295(21) | 2483-91 | 2006 |
| Tateoka K, Ouchi A, Waka M, Nakata K, Nagase D, Shimizume K, Saikawa T, <u>Hareyama M</u> | Dosimetric properties of the liquid ionization chamber electronic portal imaging device (EPID). | Igaku Butsuri | 26(1) | 28-38 | 2006 |
| Sakata K, Fuwa N, Kodaira T, Aratani K, Ikeda H, Takagi M, Nishio M, Satoh M, Nakamura S, Satoh H, <u>Hareyama M</u> . | Analyses of dose-response in radiotherapy for patients with mature T/NK-cell lymphomas according to the WHO classification | Radiother Oncol | 79(2) | 179-84 | 2006 |
| Sato Y, Takayama T, Sagawa T, Okamoto T, Miyanishi K, Sato T, Araki H, Iyama S, Abe S, Murase K, Takimoto R, Nagakura H, <u>Hareyama M</u> , Kato J, Niitsu Y. | A phase I/II study of nedaplatin and 5-fluorouracil with concurrent radiotherapy in patients with esophageal cancer. | Cancer Chemother Pharmacol | 58(5) | 570-6 | 2006 |
| Nakamura K, Shioyama Y, Kawashima M, Saito Y, Nakamura N, Nakata K, <u>Hareyama M</u> , Takada T, Karasawa K, Watanabe T, Yorozu A, Tachibana H, Suzuki G, Hayabuchi N, Toba T, Yamada S | Multi-institutional analysis of early squamous cell carcinoma of the hypopharynx treated with radical radiotherapy. | Int J Radiat Oncol Biol Phys | 65(4) | 1045-1050 | 2006 |
| 五味光太郎, 小塚拓洋, 田原誉敏, 熊田まどか, 大城佳子, <u>山下孝</u> | 肺転移に対する放射線治療 | 臨床消化器内 | 21(3) | | 2006 |
| Jingu K, Nemoto K, Matsushita H, Takahashi C, Ogawa Y, Sugawara T, Nakata E, Takai Y, <u>Yamada S</u> . | Results of radiation therapy combined with nedaplatin (cis-diammine-glycopolatinum) and 5-fluorouracil for postoperative locoregional recurrent esophageal cancer. | BMC Cancer | | | 2006 |
| Takeda K, Nemoto K, Saito H, Ogawa Y, Takai Y, <u>Yamada S</u> . | Predictive factors for acute esophageal toxicity in thoracic radiotherapy. | Tohoku J Exp Med | 208(4) | 299-306 | 2006 |

| 発表者氏名 | 論文タイトル名 | 発表誌名 | 巻号 | ページ | 出版年 |
|---|--|------------------------------|-------|-----------|------|
| Jingu K, Kaneta T, Nemoto K, Ichinose A, Oikawa M, Takai Y, Ogawa Y, Nakata E, Sakayauchi T, Takai K, Sugawara T, Narazaki K, Fukuda H, Takahashi S, <u>Yamada S.</u> | The utility of 18F-fluorodeoxyglucose positron emission tomography for early diagnosis of radiation-induced myocardial damage. | Int J Radiat Oncol Biol Phys | 66(3) | 845-851 | 2006 |
| Nakata E, Fukushima M, Takai Y, Nemoto K, Ogawa Y, Nomiya T, Nakamura Y, Milas L, <u>Yamada S.</u> | S-1, an oral fluoropyrimidine, enhances radiation response of DLD-1/FU human colon cancer xenografts resistant to 5-FU. | Oncol Rep | 16(3) | 465-471 | 2006 |
| <u>山田章吾</u> | 早期の癌に対する標準的放射線治療方法確立のための研究 | INNERVISION | 21(7) | 25 | 2006 |
| 高井憲司 | 能動的呼吸制御装置を用いた肺癌定位放射線治療 | 日放腫会誌 | 18 | 91-98 | 2006 |
| <u>大西洋</u> | 体幹部(主に肺)の定位放射線治療 | 日本放射線技術学会誌 | 62 | 661-669 | 2006 |
| <u>大西洋</u> | 放射線治療分野におけるドクターフィについて | 臨床画像 | 22 | 1162-1169 | 2006 |
| <u>大西洋</u> 、佐野尚樹、萬利乃寛、他 | 肺:呼吸性移動対策なしでは語れない「肺癌放射線治療の今」. | 映像情報 | 38 | 1157-1165 | 2006 |
| <u>大西洋</u> 、 <u>永田靖</u> 、 <u>平岡真寛</u> 、他. | I期非小細胞肺癌に対する定位放射線治療—日本多施設共同研究グループの14施設300症例の成績 | 臨床放射線 | 51 | 1145-1153 | 2006 |
| <u>大西洋</u> 、佐野尚樹、荒木力. | 体幹部定位放射線治療—その革命的意義の現状と将来 | 臨床放射線 | 51 | 583-595 | 2006 |

| 発表者氏名 | 論文タイトル名 | 発表誌名 | 巻号 | ページ | 出版年 |
|--|--|----------------------|----------|-----------|------|
| Takeda, A., Takahashi, M., Kunieda, E., Takeda, T., Sanuki, N., Koike, Y., Atsukawa, K., Ohashi, T., Saito, H., Shigematsu, N. & <u>Kubo, A.</u> | Hypofractionated stereotactic radiotherapy with and without transarterial chemoembolization for small hepatocellular carcinoma not eligible for other ablation therapies: preliminary results for efficacy and toxicity. | Hepatology Research | In press | | 2007 |
| Kunieda, E., Deloar, H.M., Takagi, S., Sato, K., Kawase, T., Saitoh, H., Saito, K., Sato, O., Sarell, G. & <u>Kubo, A.</u> | Interface software for DOSXYZnrc Monte Carlo Dose Evaluation on a Commercial RTP System. | Radiat Med | In press | | 2007 |
| Shigematsu N, Takeda A, Sanuki N, Fukada J, Uno T, Ito H, Kawaguchi O, Kunieda E, <u>Kubo A.</u> | Radiation therapy after breast-conserving surgery. | Radiat Med | 24 | 388-404 | 2006 |
| Nakahara T, Shigematsu N, Fujii M, Kunieda E, Suzuki T, Tanaka C, Hashimoto J, <u>Kubo A.</u> | Value of CT thallium-201 SPECT fusion imaging over SPECT alone for detection and localization of nasopharyngeal and maxillary cancers. | AJR Am J Roentgenol | 187 | 825-9 | 2006 |
| Kunieda E, Deloar HM, Kitamura M, Kawaguchi O, Shiba H, Takeda A, Kawase T, Seki S, Shigematsu N, <u>Kubo A.</u> | Rotational and translational reproducibility of newly developed Leksell frame-based relocatable fixation system. | Radiat Med | 24 | 503-10 | 2006 |
| Deloar HM, Kunieda E, Kawase T, Tsunoo T, Saitoh H, Ozaki M, Saito K, Takagi S, Sato O, Fujisaki T, Myojoyama A, Sorell G. | Investigations of different kilovoltage x-ray energy for three-dimensional converging stereotactic radiotherapy system: Monte Carlo simulations with CT data. | Medical Physics | 33 | 4635-4642 | 2006 |
| Kitagawa Y, Saha S, <u>Kubo A</u> , Kitajima M. | Sentinel node for gastrointestinal malignancies. | Surg Oncol Clin N Am | 16 | 71-80 | 2007 |
| Xia H, <u>Karasawa K</u> , Hanyu N, Chang TC, Okamoto M, Kiguchi Y, Kawakami M, Itazawa T. | Hyperthermia combined with intrathoracic chemotherapy and radiotherapy for malignant pleural mesothelioma. | Int J Hyperthermia | 22 | 613-21 | 2006 |
| <u>唐澤克之</u> | 肺癌の放射線治療 | 画像診断 | 26 | 1088-94 | 2006 |

| 発表者氏名 | 論文タイトル名 | 発表誌名 | 巻号 | ページ | 出版年 |
|--|--|---------------------------------|-------------|-----------|------|
| 岡本雅彦 唐澤克之 | 肺腫瘍に対する定位放射線療法 | Rad Fan | 4(8) | 35-37 | 2006 |
| 唐澤克之 羽生菜穂子 張大鎮 岡本雅彦 木口由利絵 | 当院における早期非小細胞肺癌の 三次元放射線治療と体幹部定位照 射の将来の展望 | 臨床放射線 | 51 | 1155-63 | 2006 |
| Nihei K, Ogino T, <u>Ishikura S</u> , Nishimura H. | High-dose proton beam therapy for Stage I non-small-cell lung cancer. | Int J Radiat Oncol Biol Phys | 65 | 107-111 | 2006 |
| <u>Nakamura K</u> , Shioyama Y, Nomoto S, Ohga S, Toba T, Yoshitake T, Anai S, Terashima H, Honda H. | Reproducibility of the abdominal/ chest wall position by voluntary breath-hold technique using a laser- based monitoring and visual feedback system. | Int J Radiat Oncol.Biol.Phys | 68(1) | 267-72 | 2007 |
| 椎木健裕、 <u>中村和正</u> 、他. | 肺腫瘍に対する体幹部定位放射線 治療における回転原体照射法の有 用性の検討. | 臨床放射線 | In press | | 2007 |
| 小久保 雅樹, <u>平岡 真寛</u> | 肺腫瘍に対する定位放射線治療 | 日本胸部臨床 | 第65巻増 刊号 | S275-S281 | 2006 |
| Yuichiro Kamino, Sadao Miura, <u>Masaki Kokubo</u> , Ichirou Yamashita, Etsuro Hirai, <u>Masahiro</u> <u>Hiraoka</u> , Junzo Ishikawa | Development of an ultra-small C- band linear accelerator guide for a four-dimensional image-guided radiotherapy system with a gimbaled X-ray head. | Med Phys | In Press | | 2007 |

研究成果の刊行物・別刷

Dosimetric verification in participating institutions in a stereotactic body radiotherapy trial for stage I non-small cell lung cancer: Japan clinical oncology group trial (JCOG0403)

Teiji Nishio¹, Etsuo Kunieda², Hiroki Shirato³, Satoshi Ishikura¹, Hiroshi Onishi⁴, Kunihiko Tateoka⁵, Masahiro Hiraoka⁶, Yuichirou Narita⁶, Masataka Ikeda¹ and Tomonori Goka¹

¹ Radiation Oncology Division, National Cancer Center Hospital East, Kashiwa, Japan

² Department of Radiology, Keio University, Tokyo, Japan

³ Department of Radiology, Hokkaido University Graduate School of Medicine, Sapporo, Japan

⁴ Department of Radiology, School of Medicine, University of Yamanashi, Yamanashi, Japan

⁵ Department of Radiology, Sapporo Medical University Hospital, Sapporo, Japan

⁶ Department of Therapeutic Radiology and Oncology, Kyoto University Graduate School of Medicine, Kyoto, Japan

Received 15 June 2006, in final form 6 September 2006

Published 6 October 2006

Online at stacks.iop.org/PMB/51/5409

Abstract

A multicentre phase II trial of stereotactic body radiotherapy for T1N0M0 non-small cell lung cancer was initiated in Japan as the Japan Clinical Oncology Group trial (JCOG0403). Before starting the trial, a decision was made to evaluate the treatment machine and treatment planning in participating institutions to minimize the variations of the prescription dose between the institutions. We visited the 16 participating institutions and examined the absolute dose at the centre of a simulated spherical tumour of 3.0 cm diameter in the lung using the radiation treatment planning systems in each institution. A lung phantom for stereotactic body radiotherapy (SBRT) was developed and used for the treatment planning and film dosimetry. In the JCOG radiotherapy study group, the no model-based calculation algorithm or the model-based calculation algorithm with a dose kernel unscaled for heterogeneities were selected for use in the initial SBRT trials started in 2004, and the model-based calculation algorithm with a dose kernel scaled for heterogeneities was selected for the coming trial. The findings of this study suggest that the clinical results of lung SBRT trials should be carefully evaluated in comparison with the actual dose given to patients.

1. Introduction

With recent technological advances in computed tomography (CT) apparatuses, the detection of early lung cancer has been markedly increasing. The technology of high-accuracy radiotherapy, which focuses the radiation on the tumour, has rapidly developed in Japan and other countries. Stereotactic body radiotherapy (SBRT) is one type of high-accuracy radiotherapy and has been developed since the 1990s and applied to lung cancer treatment (Blomgren *et al* 1995, Uematsu *et al* 1996).

As SBRT has been covered by the national health insurance system in Japan since 2004, the number of institutions performing SBRT is rapidly increasing. The reference for the set-up can be bone structures, internal fiducial markers, or the tumour itself. Two orthogonal megavoltage or kilo-voltage x-ray images or CT scans in the treatment room can be used to detect the reference structure. Various solutions for the determination of internal target volume are available. Generally, SBRT is performed with a high daily dose of 5–12 Gy with a small number of 4–10 fractions within 2 weeks, giving more than 80 Gy of biological equivalent dose (BED) without cell proliferation assuming an α/β rate of 10. Multi-port irradiation or arc irradiation using a multi-leaf collimator (MLC) is the most common technique. The treatment duration is about 1 h, during which the set-up of the patient and its verification are the most time consuming.

Especially for stage IA disease, the local control rate is more than 90% in most series with the 5 year survival rate being much better than that reported with conventional radiotherapy in the literature (Uematsu *et al* 2001, Nakagawa *et al* 2000, Fukumoto *et al* 2002, Nagata *et al* 2002, Onimaru *et al* 2003, Timmerman *et al* 2003, Onishi *et al* 2004). The apparent superiority may be exaggerated by the stage migration in the retrospective comparison because of the advances in CT and positron emission tomography (PET), allowing them to detect smaller tumours. However, the short course of treatment with the minimal adverse effect of SBRT seems to be a sufficient advantage so that SBRT can be a good alternative to conventional radiotherapy in clinical practice (Fowler *et al* 2004).

One problem is that since each institution has used a different treatment schedule, there has been no standard schedule to be recommended in guidelines (JASTRO QA committee ?). Furthermore, the definitions of the prescribed dose, selection of set-up error and dose calculation algorithm have not been standardized, so that comparison between different institutions was impossible. In 2003, therefore, we, the Japan Clinical Oncology Group (JCOG), decided to perform multi-institutional trials to test the efficacy of SBRT with a precise quality control study.

In this study, to improve the quality control, we made a comparative study of the dosimetric parameters in the various institutions that are involved in the clinical study of SBRT. Since many Japanese institutions have used the central dose, not the peripheral dose, as the prescription point for SBRT, we have tested the consistency of the absolute dose at the centre of the simulated tumour in a lung phantom in this study.

2. Materials and methods

We visited the 16 institutions which were participating in the clinical trial and examined various parameters using a phantom specially made for lung SBRT (Deloar *et al* 2005) (figure 1). Irradiation field size, the dose uniformity in the rectangular field and the irradiation dose were measured and compared with those calculated using the institutional calculation algorithm for SBRT in the radiation treatment planning system (RTP). The RTPs tested in this study were FOCUS/XiO (CMS Inc., St Louis, MO, USA), CADPlan/ECLIPSE (Varian Medical

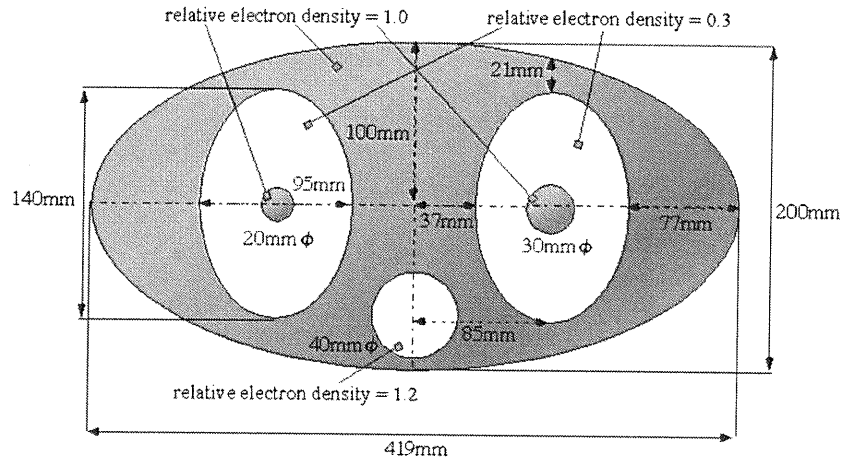


Figure 1. Lung phantom designed for SBRT.

Systems Inc., Palo Alto, CA, USA), Pinnacle³ (Philips Medical Systems Inc., Eindhoven, The Netherlands), PrecisePLAN (Elekta Corp., Stockholm, Sweden), and RPS700U (Mitsubishi Electric Co. Ltd., Tokyo, Japan). The measurement was performed using a film dosimetric method previously reported by other investigators (Childress *et al* 2002, Childress and Rosen 2004, Childress *et al* 2005a, 2005b, 2005c, Bucciolini *et al* 2004, Gorny *et al* 2005, Hirata *et al* 2005).

2.1. Lung phantom designed for SBRT and film dosimetric verification system

Heterogeneity in the lung phantom shown in figure 1 was constructed with water equivalent (tough water: physical density 1.0 g cm^{-3}), lung equivalent (tough lung: physical density 0.3 g cm^{-3}), and bone equivalent (BE-H tough bone: physical density 1.5 g cm^{-3}) phantoms (KYOTO KAGAKU Co. Ltd, Kyoto, Japan). The relative electron density of the thoracic wall and of the simulated tumours with a 20 mm diameter and 30 mm diameter was 1.0. EDR2 film (Kodak Inc., New York, USA) was used as the dosimetric film in this study. The film can be inserted into the phantom crossing at the centre of the simulated tumour. A homemade device was used to press the film and the phantom in order to decrease the gap between them. The actual dose used to irradiate the film was decided using an air chamber calibrated with a ^{60}Co -gamma ray source in the Secondary Standard Dosimetry Laboratory (SSDL) of Japan. The irradiated film was scanned with 100 dpi and a 14 bit greyscale by using a commercially available image-scanner: ES-8500 (EPSON Corp., Nagano, Japan). Analysis of the irradiated film was performed using a commercially available densitometer, DD system (R'Tech Inc., Tokyo, Japan). The film dosimetric method was adopted for verification of the absolute dose because dose measurement with high accuracy in a tumour of small size using the ionization chamber with large effective volume is difficult and the dosimetric film has an accuracy of dose measurement within 2% by taking the calibration curve in each film processing.

2.2. Method of evaluation of the absolute dose calculated using the RTPs

CT images of the lung phantom were taken under the same conditions as used in each institution for SBRT. Imaging was performed by positioning the centre of the simulated tumour at the

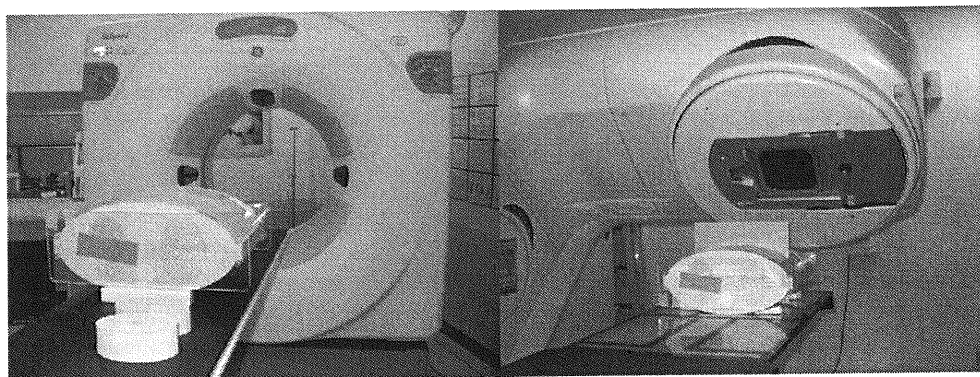


Figure 2. CT imaging and film irradiation using the lung phantom for SBRT.
(This figure is in colour only in the electronic version)

centre of the CT slice thickness with no synchronous movement of the phantom. The treatment planning was performed using the RTPs owned by each institution. The calculation algorithms were categorized into two types. The type-B calculation algorithm is model-based and uses a dose kernel that is scaled in each voxel to account for heterogeneities. The others can be summarized as the type-A calculation algorithms. The gross tumour volume (GTV) was established to be consistent with the simulated spherical tumour with a diameter of 30 mm on the CT images. In addition, the clinical target volume (CTV) with a three-dimensional 5 mm margin from the GTV and planning target volume (PTV) with a three-dimensional 5 mm margin from the CTV were defined. These were grossly consistent with the clinical practice. The edge of the multi-leaf collimator (MLC) was set at the PTV. Overall, a beam with a 50 mm diameter 50% isodose line at the isocentre was used to irradiate the tumour although various types of collimators were used in the 16 institutions. In the treatment plan, the therapeutic beam was delivered to the PTV with a gantry angle of 2° to the body axis of the phantom (2° to prevent leakage of the beam into the gap between the parts of phantom for film dosimetry) and with a gantry angle of 45° . They were defined by the plan names of 'plan 1' and 'plan 2', respectively.

The dosimetric film was placed at the centre of the simulated tumour in the phantom, and irradiation was performed at 200 MU using plans 1 and 2. Figure 2 shows CT scanning and irradiation of the film using the lung phantom. We also performed processing of all irradiated films in our centre. The irradiated films were scanned using an ES-8500 image-scanner and analysed using a DD system.

3. Results

3.1. Conversion from film optical density to the dose of the dosimetric film

Figure 3 shows the relationship between the radiation dose and film optical density for all participating institutions. These data were obtained by processing the dosimetric film irradiated in different institutions on different days. The high reproducibility of the results indicates that the maintenance of the film processing device was executed with reliable quality. In the figure, the characteristic curve was observed to divide roughly into two. The verification of the absolute dose was performed by doses of about 1.5, 1.6 and 1.7 Gy converted from 200 MU value at 4, 6 and 10 MV, respectively.

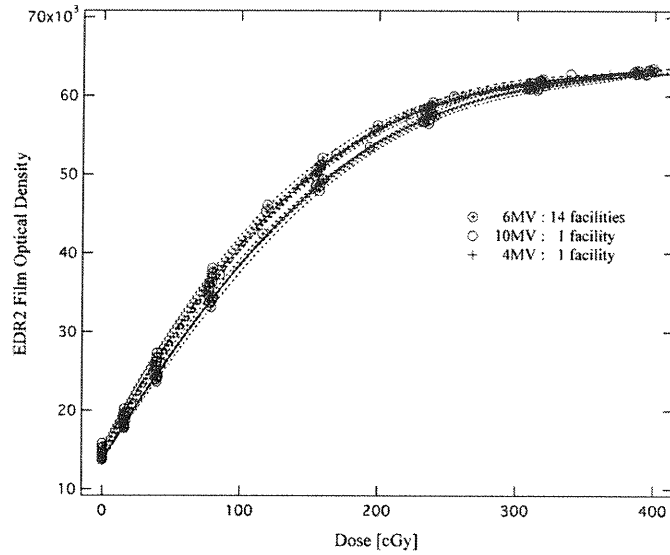


Figure 3. Relationship between the radiation dose and film optical density in the 16 participating institutions.

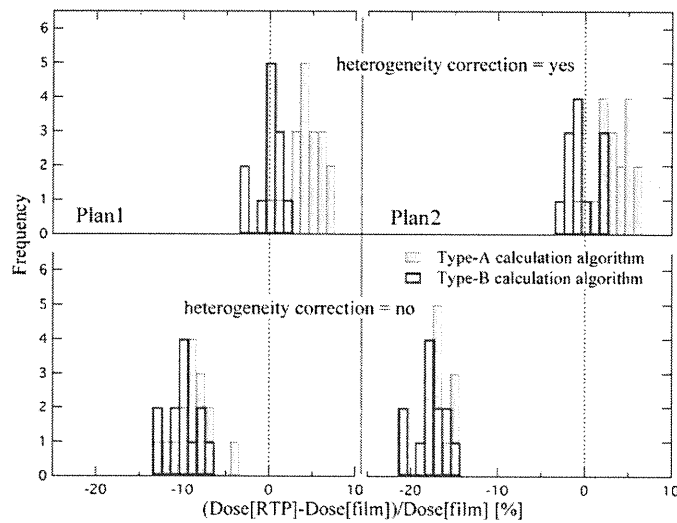


Figure 4. Differences between the dose measured with the dosimetric film and that calculated by using the type-A and -B calculation algorithms with/without the heterogeneity correction effect by irradiation at 200 MU in plans 1 and 2.

3.2. Evaluation of the absolute dose calculated using the RTPs

Figure 4 illustrates the frequency distribution of the discrepancy between the actual point dose estimated by film dosimetry and the planned dose in RTPs at the central point of the irradiation field that was at the centre of the simulated tumour in the phantom. With heterogeneity correction, the type-B calculation algorithms produced better matches with the film dosimetry

Table 1. Summary of the differences between the dose measured with the dosimetric film and that calculated by using the indicated calculation algorithms in RTPs.

| Institutions | Energy (MV) | RTP system | Type-A calculation algorithm | | | | Type-B calculation algorithm | | | |
|--------------|-------------|-----------------|------------------------------|-----------------------------|--------|--------------------|------------------------------|--------|--|--|
| | | | Algorithm | Difference (%) ^a | | Algorithm | Difference (%) ^a | | | |
| | | | | Plan 1 | Plan 2 | | Plan 1 | Plan 2 | | |
| A | 6 | FOCUS/XiO | Clarkson | 4 | 3 | Superposition | 1 | -1 | | |
| | | Pinnacle3 | CC (hetero/homo) | 6 | 4 | CC (hetero/hetero) | 0 | -2 | | |
| B | 6 | FOCUS/XiO | Clarkson | 5 | 5 | Superposition | 1 | 0 | | |
| C | 6 | FOCUS/XiO | Clarkson | 1 | 2 | Superposition | -3 | -3 | | |
| D | 6 | FOCUS/XiO | Clarkson | 3 | 3 | Superposition | 0 | -1 | | |
| E | 10 | FOCUS/XiO | Clarkson | 4 | 1 | Superposition | 0 | 2 | | |
| F | 6 | CADPlan/ECLIPSE | Batho | 3 | 2 | | | | | |
| G | 6 | CADPlan/ECLIPSE | Batho | 0 | 4 | | | | | |
| H | 6 | Pinnacle3 | CC (hetero/homo) | 7 | | CC (hetero/hetero) | 2 | 2 | | |
| I | 6 | PrecisePlan | Area Integration | 3 | -1 | | | | | |
| | | CADPlan/ECLIPSE | Batho | 4 | 2 | | | | | |
| J | 6 | RPS700U(3D) | Ratio TPR | 6 | 6 | | | | | |
| | | Pinnacle3 | CC (hetero/homo) | 7 | 5 | CC (hetero/hetero) | 1 | -1 | | |
| K | 6 | FOCUS/XiO | Clarkson | 4 | 6 | Superposition | 0 | 2 | | |
| L | 6 | Pinnacle3 | CC (hetero/homo) | 5 | | CC (hetero/hetero) | 0 | -2 | | |
| M | 6 | CADPlan/ECLIPSE | Batho | 4 | 3 | | | | | |
| N | 6 | FOCUS/XiO | Clarkson | 5 | 5 | Superposition | -1 | -1 | | |
| O | 6 | CADPlan/ECLIPSE | Batho | 4 | 2 | | | | | |
| | | FOCUS/XiO | Clarkson | 2 | 3 | Superposition | -3 | -2 | | |
| P | 4 | | Median | 4 | 3 | | 0 | -1 | | |
| | | | Max | 7 | 6 | | 2 | 2 | | |
| | | | Min | 0 | -1 | | -3 | -3 | | |
| | | | SD | 2 | 2 | | 2 | 2 | | |

a $\frac{(\text{Calculated dose}) - (\text{Measured dose})}{(\text{Calculated dose})} \times 100$.

than the type-A calculation algorithms for both plan 1 and for plan 2 (upper two figures in figure 4). Without heterogeneity correction, the modes of planned dose were 10% lower for plan 1 and 18% lower for plan 2, respectively, and no apparent difference was observed between the two algorithms (lower two figures in figure 4). The range of the differences between the calculated dose and the measured dose is shown in table 1. The difference in the absolute dose calculated with each calculation algorithm was within 7% among the 16 participating institutions, irrespective of whether it was calculated with/without the heterogeneity correction effect in plans 1 and 2, with both showing a similar tendency. There was no difference in the calculated absolute dose between the algorithms regardless of the correction effect.

Table 1 shows a summary of the discrepancy between the dose at the isocentre measured with the dosimetric film and that calculated with each of the calculation algorithms in all of the 16 participating institutions. In the table, the discrepancy between the dose calculated using the type-A and -B calculation methods and the dose estimated from film densitometry is shown in each column. The median of the differences in the absolute dose determined using the type-A calculation algorithm was +4%, and that determined using the type-B calculation algorithm was -1%, the difference between them being 5%. The standard deviation was 2% using both the type-A and -B calculation algorithms in each plan.

4. Discussion and conclusions

The method of verification of dosimetry using a lung phantom for SBRT and dosimetric film was shown here to be useful for dosimetric verification in multiple institutions. The effect of heterogeneity correction on biasing the dose in lung SBRT was clearly demonstrated with the phantom experiment in this study. However, the effect of the respiratory motion of the organ was not verified in this study. The research of the consequence is an important topic in the future. Based on this study, we have decided to use heterogeneity correction in the JCOG0403 study of SBRT for stage I non-small cell lung cancer. The prescription total dose of 48 Gy at isocentre is performed with a daily dose of 12 Gy in 4 fractions within 2 weeks. The MLC margin is set from the PTV line by 5 mm for the 95% coverage of PTV. Since the RTOG0236 trial of SBRT for lung tumours, which was based on the trial at Indiana University (McGarry *et al* 2005), is not using heterogeneity correction in their protocol, it is important to realize that the actual dose in the RTOG0236 trial would be higher than that in the JCOG0403 study. The findings of our experiment with the phantom suggested that the difference due to the lack of a heterogeneity correction for SBRT of small lung tumours would be as large as 10 to 18%.

The discrepancy between the calculated and measured doses in the RTPs was +4% for the type-A calculation algorithm and -1% for the type-B calculation algorithm in our phantom study. The calculated result by the type-B calculation algorithm reproduced the measured result with higher accuracy. The standard deviation of the differences among institutions regarding the discrepancy between the calculated and measured dose was the same for the two calculation algorithms whether the heterogeneity correction was used or not.

The type-B algorithm was more accurate than other algorithms. However, we have decided to use the type-A calculation algorithm with heterogeneity correction effect in the initial clinical trial for SBRT, JCOG0403, for stage IA non-small cell lung cancer. The reasons for the selection of the type-A algorithm instead of the type-B calculation algorithm were that RTPs with the type-B calculation algorithm were not available in some participating institutions (CADPlan/ECLIPSE users) at the time when the trial was started, and the regulations of the absolute dose were all based on clinical data obtained using the type-A calculation algorithm with heterogeneity correction effect (Fukumoto *et al* 2002, Nagata *et al* 2002, Onishi *et al* 2004). Since we used fixed irradiation conditions with the phantom in this study, differences would be larger in clinical situations. Therefore, in addition to this investigation, it is also important to perform many verification tests for treatment planning under various conditions in each participating institution. Based on this study, we have decided to use the type-B calculation method with heterogeneity correction in the upcoming clinical trial of SBRT for T2 diseases. This is consistent with the recommendation in Report No 85 by AAPM TG65 (AAPM 2004).

Lung SBRT is often characterized by parameters such as the dose at the periphery of the tumour, D95 of PTV (dose of the 95% PTV volume), the mean dose to the lung, V20 (volume of the entire lung irradiated by more than 20 Gy in total), HI (homogeneity index), which is a parameter of the homogeneity within the PTV and CI (conformity index), representing the rate of unnecessary irradiation areas (ICRU ?). We did not examine the dose at the periphery of the PTV in this study. If we examine the dose at the periphery of the PTV, the difference in dose calculated using different algorithms and heterogeneity correction will be larger and more variable. In fact, there was a difference in the prescription point between the RTOG0236 trial for SBRT and the JCOG0403 trial. In the former, the peripheral dose without heterogeneity correction was used and in the latter, the isocentre with heterogeneity correction was used as the prescription point. The finding of this study suggests that the clinical results of

these trials should be carefully compared and dose–volume histogram (DVH) analysis should be carefully interpreted.

Acknowledgments

We would like to thank the medical physicists and the staff of the institutions who helped us during the visiting survey. We would also like to thank the members of the JCOG radiotherapy study group for suggestions. We greatly appreciate the radiotherapy technologists at the National Cancer Centre Hospital East for helping us to study the film characteristics.

References

- AAPM TG65 2004 Tissue inhomogeneity corrections for megavoltage photon beams *AAPM Report No 85* (College Park, MD: AAPM)
- Blomgren H, Lax I, Naslund I and Svanstrom R 1995 Stereotactic high dose fraction radiation therapy of extracranial tumors using an accelerator. Clinical experience of the first thirty-one patients *Acta Oncol. Biol. Phys.* **34** 861–70
- Bucciolini M, Buonamici F B and Casati M 2004 Verification of IMRT fields by film dosimetry *Med. Phys.* **31** 161–8
- Childress N L, Dong L and Rosen I I 2002 Rapid radiographic film calibration for IMRT verification using automated MLC fields *Med. Phys.* **29** 2384–90
- Childress N L and Rosen I I 2004 Effect of processing time delay on the dose response of Kodak EDR2 film *Med. Phys.* **31** 2284–8
- Childress N L, Bloch C, White R A, Salehpour M and Rosen I I 2005a Detection of IMRT delivery errors using a quantitative 2D dosimetric verification system *Med. Phys.* **32** 153–62
- Childress N L, Salehpour M, Dong L, Bloch C, White R A and Rosen I I 2005b Dosimetric accuracy of Kodak EDR2 film for IMRT verifications *Med. Phys.* **32** 539–48
- Childress N L, White R A, Bloch C, Salehpour M, Dong L and Rosen I I 2005c Retrospective analysis of 2D patient-specific IMRT verifications *Med. Phys.* **32** 838–50
- Deloar H M et al 2005 Investigations of suitable kilo-voltage x-ray energy for 3DCRT system with Monte Carlo simulations *14th Int. Conf. of Medical Physics (Nuremberg, Germany)* pp 1057–8
- Fowler J F, Tome W A, Fenwick J D and Mehta M P 2004 A challenge to traditional radiation oncology *Int. J. Radiat. Oncol. Biol. Phys.* **60** 1241–56
- Fukumoto S, Shirato H, Shimizu S, Ogura S, Onimaru R, Kitamura K, Yamazaki K, Miyasaka K, Nishimura M and Dosaka-Akita H 2002 Small-volume image-guided radiotherapy using hypofractionated, coplanar, and noncoplanar multiple fields for patients with inoperable stage I non-small cell lung carcinomas *Cancer* **95** 1546–53
- Gorny K R, Leitzner S L, Bruesewitz M R and Kofler J M 2005 The calibration of experimental self-developing Gafchromic HXR film for the measurement of radiation dose in computed tomography *Med. Phys.* **32** 1010–6
- Hirata E Y, Cunningham C, Micka J A, Keller H, Kissick M W and DeWerd L A 2005 Low dose fraction behavior of high sensitivity radiochromic film *Med. Phys.* **32** 1054–60
- ICRU 1999 Prescribing, recording, and reporting photon beam therapy *ICRU Report 62* (Bethesda, MD: ICRU) (supplement to ICRU Report 50)
- Japanese Society for Therapeutic Radiology and Oncology QA committee 2006 Guideline for stereotactic body radiotherapy *J. Japan. Soc. Ther. Radiol. Oncol.* **18** 1–17 (<http://www.jastro.jp/guideline/files/SRT.pdf>)
- McGarry R C, Papiez L, Williams M, Whitford T and Timmerman R D 2005 Stereotactic body radiation therapy of early-stage non-small-cell lung carcinoma: phase I study *Int. J. Radiat. Oncol. Biol. Phys.* **63** 1010–5
- Nakagawa K, Aoki Y, Tago M, Terahara A and Ohtomo K 2000 Megavoltage CT-assisted stereotactic radiosurgery for thoracic tumors: original research in the treatment of thoracic neoplasms *Int. J. Radiat. Oncol. Biol. Phys.* **48** 449–57
- Nagata Y et al 2002 Clinical outcomes of 3D conformal hypofractionated single high-dose radiotherapy for one or two lung tumors using a stereotactic body frame *Int. J. Radiat. Oncol. Biol. Phys.* **52** 1041–6
- Onimaru R et al 2003 Tolerance of organs at risk in small-volume, hypofractionated, image-guided radiotherapy for primary and metastatic lung cancers. *Int. J. Radiat. Oncol. Biol. Phys.* **56** 126–35
- Onishi H, Kuriyama K, Komiyama T, Tanaka S, Sano N, Marino K, Ikenaga S, Araki T and Uematsu M 2004 Clinical outcomes of stereotactic radiotherapy for stage I non-small cell lung cancer using a novel irradiation technique: patient self-controlled breath-hold and beam switching using a combination of linear accelerator and CT scanner *Lung Cancer* **45** 45–55

- Onishi H *et al* 2004 Stereotactic hypofractionated high-dose irradiation for stage I non-small cell lung carcinoma: clinical outcomes in 245 subjects in a Japanese multiinstitutional study *Cancer* **101** 1623–31
- Timmerman R, Papiez L, McGarry R, Likes L, DesRosiers C, Frost S and Williams M 2003 Extracranial stereotactic radiation: results of a phase I study in medically inoperable stage I non-small cell lung cancer *Chest* **124** 1946–55
- Uematsu M, Fukui T, Shioda A, Tokumitsu H, Takai K, Kojima T, Asai Y and Kusano S 1996 A dual computed tomography linear accelerator unit for stereotactic radiation therapy: a new approach without cranially fixated stereotactic frames *Int. J. Radiat. Oncol. Biol. Phys.* **35** 587–92
- Uematsu M, Shioda A, Suda A, Fukui T, Ozeki Y, Hama Y, Wong J R and Kusano S 2001 Computed tomography-guided frameless stereotactic radiotherapy for stage I non-small-cell lung cancer: a 5-year experience *Int. J. Radiat. Oncol. Biol. Phys.* **51** 666–70



ELSEVIER

doi:10.1016/j.ijrobp.2006.12.046

PHYSICS CONTRIBUTION

REPRODUCIBILITY OF THE ABDOMINAL AND CHEST WALL POSITION BY VOLUNTARY BREATH-HOLD TECHNIQUE USING A LASER-BASED MONITORING AND VISUAL FEEDBACK SYSTEM

KATSUMASA NAKAMURA, M.D.,* YOSHIYUKI SHIOYAMA, M.D.,* SATORU NOMOTO, M.D.,* SAJI OHGA, M.D.,* TAKASHI TOBA, M.D.,* TADAMASA YOSHITAKE, M.D.,* SHIGEO ANAI, R.T.T.,† HIROMI TERASHIMA, M.D.,‡ AND HIROSHI HONDA, M.D.*

*Department of Clinical Radiology, Graduate School of Medical Sciences, †Radiology Center, and ‡Department of Health Sciences, School of Medicine, Kyushu University, Fukuoka, Japan.

Purpose: The voluntary breath-hold (BH) technique is a simple method to control the respiration-related motion of a tumor during irradiation. However, the abdominal and chest wall position may not be accurately reproduced using the BH technique. The purpose of this study was to examine whether visual feedback can reduce the fluctuation in wall motion during BH using a new respiratory monitoring device.

Methods and Materials: We developed a laser-based BH monitoring and visual feedback system. For this study, five healthy volunteers were enrolled. The volunteers, practicing abdominal breathing, performed shallow end-expiration BH (SEBH), shallow end-inspiration BH (SIBH), and deep end-inspiration BH (DIBH) with or without visual feedback. The abdominal and chest wall positions were measured at 80-ms intervals during BHs. **Results:** The fluctuation in the chest wall position was smaller than that of the abdominal wall position. The reproducibility of the wall position was improved by visual feedback. With a monitoring device, visual feedback reduced the mean deviation of the abdominal wall from 2.1 ± 1.3 mm to 1.5 ± 0.5 mm, 2.5 ± 1.9 mm to 1.1 ± 0.4 mm, and 6.6 ± 2.4 mm to 2.6 ± 1.4 mm in SEBH, SIBH, and DIBH, respectively.

Conclusions: Volunteers can perform the BH maneuver in a highly reproducible fashion when informed about the position of the wall, although in the case of DIBH, the deviation in the wall position remained substantial.
 © 2007 Elsevier Inc.

Breath-hold, Reproducibility, Gating, Radiotherapy, Visual feedback.

INTRODUCTION

In stereotactic radiotherapy for lung or liver tumors, 1 of the most important issues is to reduce respiratory motion of the target (1–3). To deliver the radiation dose to the entire volume of a moving target, various approaches have been used (4–8). The voluntary breath-hold (BH) technique is a simple method of controlling the respiration-related motion of a tumor during irradiation. In particular, the deep inspiration breath-hold (DIBH) technique has been developed and clinically implemented. Hanley *et al.* (9) demonstrated that the DIBH maneuver, conducted with a spirometer, enabled highly reproducible positions to be achieved. The results of the Hanley *et al.* study (9) have been supported by several other reports (10–12). However, Balter *et al.* (13) reported that the reproducibility of the diaphragm position was better at the expiration phase than that at the inspiration

phase when the voluntary BH technique was implemented. Using spirometer-based monitoring, Kimura and colleagues (14) demonstrated that gating in the end-expiration phase was more reproducible than gating in the end-inspiration phase. Although it remains controversial whether patients should hold their breath at the inspiration or expiration phase, the end-expiration phase seems to be more stable.

Visual feedback techniques, which may improve the potential for BH compliance, are being increasingly used in cases treated with extracranial stereotactic radiotherapy. Several studies have suggested that visual or audio feedback (or both) improves the reproducibility of the abdominal and chest wall position (15–18). Feedback-guided BH can help the patient achieve reproducibility in the BH position, which may in turn reduce the respiration-related uncertainty of the location of the target (16).

We have developed a simple device using a laser diode

Reprint requests to: Katsumasa Nakamura, Department of Clinical Radiology, Graduate School of Medical Sciences, Kyushu University, Maidashi 3-1-1, Higashi-ku, Fukuoka 812-8582, Japan. Tel. (+81) 92-642-5695; Fax (+81) 92-642-5708; E-mail: nakam@radiol.med.kyushu-u.ac.jp

Acknowledgment—This study was supported in part by the Grants-

in-Aid for Scientific Research from Japan Society for the Promotion of Sciences (Grant Nos. 15591284 and 18591383) and from the Japanese Ministry of Health, Labor and Welfare.

Conflict of interest: none.

Received Aug 5, 2006, and in revised form Nov 27, 2006.
 Accepted for publication Dec 18, 2006.

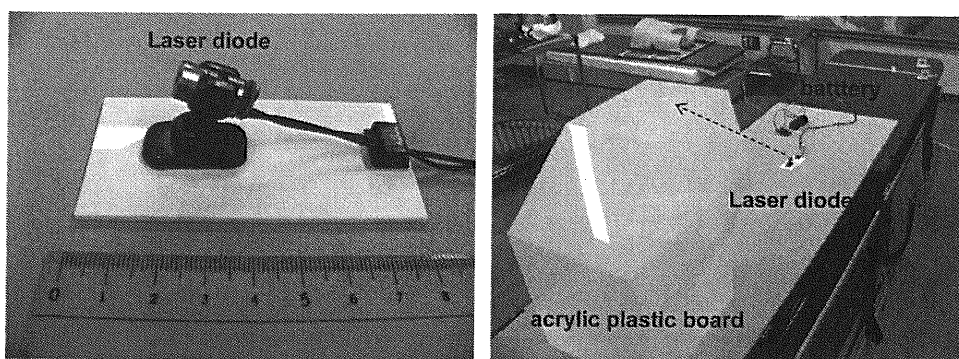


Fig. 1. The respiratory monitoring device. The system consists of a small laser diode mounted on a joint and a translucent overhead board.

resting on the abdominal wall to allow convenient respiratory monitoring by a therapist as well as the patient. The purpose of this study was to examine whether visual feedback using this device can reduce fluctuations in the position of the abdominal and chest walls during various BH maneuvers.

METHODS AND MATERIALS

Visual feedback using a new simple respiratory monitoring device

The respiratory monitoring device used in this study consists of a small laser diode and a translucent overhead board (Fig. 1). A class II laser diode with a length of less than 1.5 cm is mounted on a joint, which controls the direction of the laser beam. A translucent overhead board is set in place for the detection of the beam. Figure 2 provides a scheme for this monitoring device. A laser beam, resting on the abdominal wall, is projected onto the board above the volunteer, and this beam moves according to the respiratory cycle. A volunteer practicing abdominal breathing can control the motion of the diaphragm, because the volunteer can observe the motion of the laser beam on the board. A mark can be placed on the board to guide breath holding, pointing to the position where the BH needs to occur. A physician or therapist can also monitor the motion of the laser beam on the board using a camera mounted inside treatment room.

Measurement of the displacement of abdominal and chest walls during BHs

In general, the motion of the tumor and external patient marker were correlated (19, 20). Thus, in this study, only the chest and

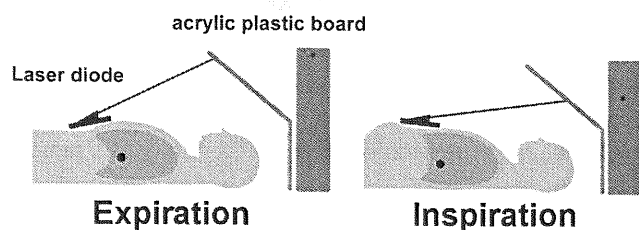


Fig. 2. A scheme of the respiratory monitoring device. For an abdominal breather, the anterior motion of the abdomen corresponds to inhalation, and the posterior motion of the abdomen corresponds to exhalation. A laser beam, projected onto the board above the volunteer, moves according to the respiratory cycle.

abdominal wall positions were measured instead of intrathoracic structures using fluoroscopy. For the detection and calculation of the abdominal and chest wall position, a commercially available high-speed machine vision system (XV-1000, Keyence, Osaka, Japan) was used (Fig. 3) (21). This machine vision system was composed of 640×480 pixel CCD cameras and computerized control systems. Two couple-charged device cameras were positioned 1.5 m from each volunteer, who assumed a supine position on the treatment couch. External fiducials (X-spots, Beekley, CT) were placed on the chest wall (at the middle of the sternum) and abdominal wall (midway between the xyphoid tip and the umbilicus) (Fig. 3). The image data obtained from the fiducials on the abdominal and chest walls were captured onto the couple-charged device, converted to digital data within the camera unit, and transferred to the controller, after which the position of the fiducials was calculated to an accuracy of <0.1 mm (21). The image data were captured, and the positions of the fiducials (i.e., the position of the wall) were calculated at 80-ms intervals during the BH. The calculation time was approximately 50 ms.

Data collection

Four healthy male volunteers and one healthy female volunteer with a median age of 26 years (range, 25–32 years) were enrolled in this study. The volunteers were placed on the treatment couch to perform several BH maneuvers. The volunteers were initially instructed to breathe with the abdomen, which means that breathing activity should be carried out mainly by the abdomen. The participants were then shown their respiratory trace on the respiratory monitoring device, which facilitated visual feedback of the information regarding the respiratory cycle. After it was confirmed that the device worked properly, the subjects were instructed to hold their breath for 15 s at the same wall position using the following BH types: end-expiration (shallow expiration breath-hold [SEBH]), end-inspiration (shallow inspiration breath-hold [SIBH]), and deep end-inspiration (deep inspiration breath-hold [DIBH]). For SEBH and SIBH, a mark was placed on the translucent overhead board at the minimum or maximum position of the beam according to the normal respiratory cycle. For DIBH, a mark was placed after coaching the volunteer to perform a reproducible DIBH. Each volunteer performed five repetitions of the same type of 15-s BH without using the present device, and then the volunteers performed the same procedures with the device. Between BHs, the volunteers breathed freely for 30–60 s.

To evaluate the reproducibility of the wall position, we measured the distance between the reference point and the wall position during each session (five repetitions of 15-s BH). Just before

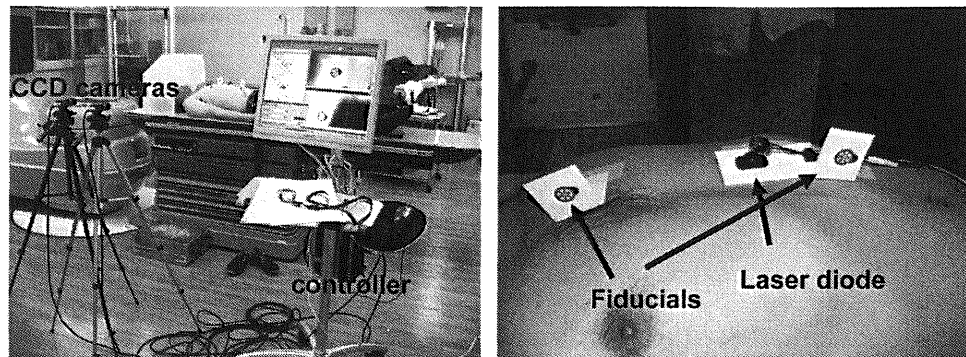


Fig. 3. Setup for visual feedback showing a volunteer viewing the laser beam on a plastic board. Two couple-charged device cameras were positioned 1.5 m from the volunteer on the treatment couch; fiducials were placed on the abdominal and chest walls of the volunteer. The image data obtained from the fiducials were transferred to the controller.

the start of the each session, the positions of the abdominal and chest walls were established as reference points for a specific respiration BH type. Then, the distance between the reference point and the wall position was calculated by the XV-1000 system at 80-ms intervals during each session. A total of more than 5,600 positions of the abdominal and chest walls were collected per volunteer.

RESULTS

Figure 4 shows an example of the fluctuation in the position of the abdominal and chest walls during five iterations of 15-s BH for three BH types. Without visual feedback, the reproducibility of the wall position in the case of SEBH and SIBH was better than that associated with DIBH. It should be noted that the abdominal wall moved during BH for all types of BH and that fluctuations in the abdominal wall position exceeded 10 mm during DIBH. However, the reproducibility of the wall position was improved by visual feedback.

Table 1 summarizes the distribution of the wall position during the session of each BH type for each of five volunteers. The fluctuation in the abdominal wall position was much larger than that of the chest wall position, partly because the volunteers had practiced abdominal breathing. Without visual feedback, the mean deviation of the abdominal wall position was smallest in the case of SEBH. However, visual feedback decreased the mean deviation in the abdominal wall position from 2.1 ± 1.3 mm to 1.5 ± 0.5 mm, 2.5 ± 1.9 mm to 1.1 ± 0.4 mm, and 6.6 ± 2.4 mm to 2.6 ± 1.4 mm in SEBH, SIBH, and DIBH, respectively. Although the device used here worked effectively, the deviation remained substantial in the case of DIBH.

DISCUSSION

In this study, we demonstrated the technical feasibility of the BH maneuver using a new respiratory monitoring device. This study suggests that visual feedback reduces wall position deviations during SEBH, SIBH, and DIBH. Although this system seemed to increase the deviation of the

chest wall position in some volunteers (Table 1), almost all of the deviations were still within 1 mm in SEBH and SIBH. However, the chest and abdominal wall deviation remained substantial in the case of DIBH. In addition, the visual feedback technique did not improve the deviation of the abdominal wall position in SEBH and DIBH in Volunteer 1. Unfortunately, all BH techniques are subject to patient compliance. The effectiveness of a BH technique should be verified before treatment in every case, because even a simple task such as a BH maneuver can be challenging for many lung cancer patients.

Visual feedback techniques are increasingly used for the treatment of patients with lung or liver tumors. Kini *et al.* (15) demonstrated that when patients were shown a real-time trace of their abdominal wall motion, the visual feedback maintained the range of respiratory motion. That study suggested that visual feedback was more successfully implemented than audio feedback in the control of the amplitude of breathing motion in most patients in respiratory-gated radiotherapy. Using a liquid crystal display screen, George *et al.* (18) concluded that audiovisual feedback significantly improved respiratory reproducibility of gating. Nelson *et al.* (16) developed a feedback-guided BH technique using a liquid crystal display or a pair of virtual reality goggles. Carlson *et al.* (17) reported that BH monitoring and feedback allowed the patient to perform reliable BH through a bellows-based monitoring system. Our study using a laser-based BH monitoring and feedback system also showed that a volunteer could perform BH accurately when the respiratory trace was shown to the volunteer. Visual feedback thus appears to be a promising means of helping patients achieve reproducibility of BH position, which may in turn lead to a reduction in the respiration-related uncertainty of a tumor's location.

Among several respiratory gating methods currently in use, the voluntary BH technique is one of the most simple for controlling respiration-related motion of a tumor during irradiation. Kimura *et al.* (14) not only demonstrated good reproducibility of the diaphragm position but also noted that this reproducibility was enhanced at the end-expiration

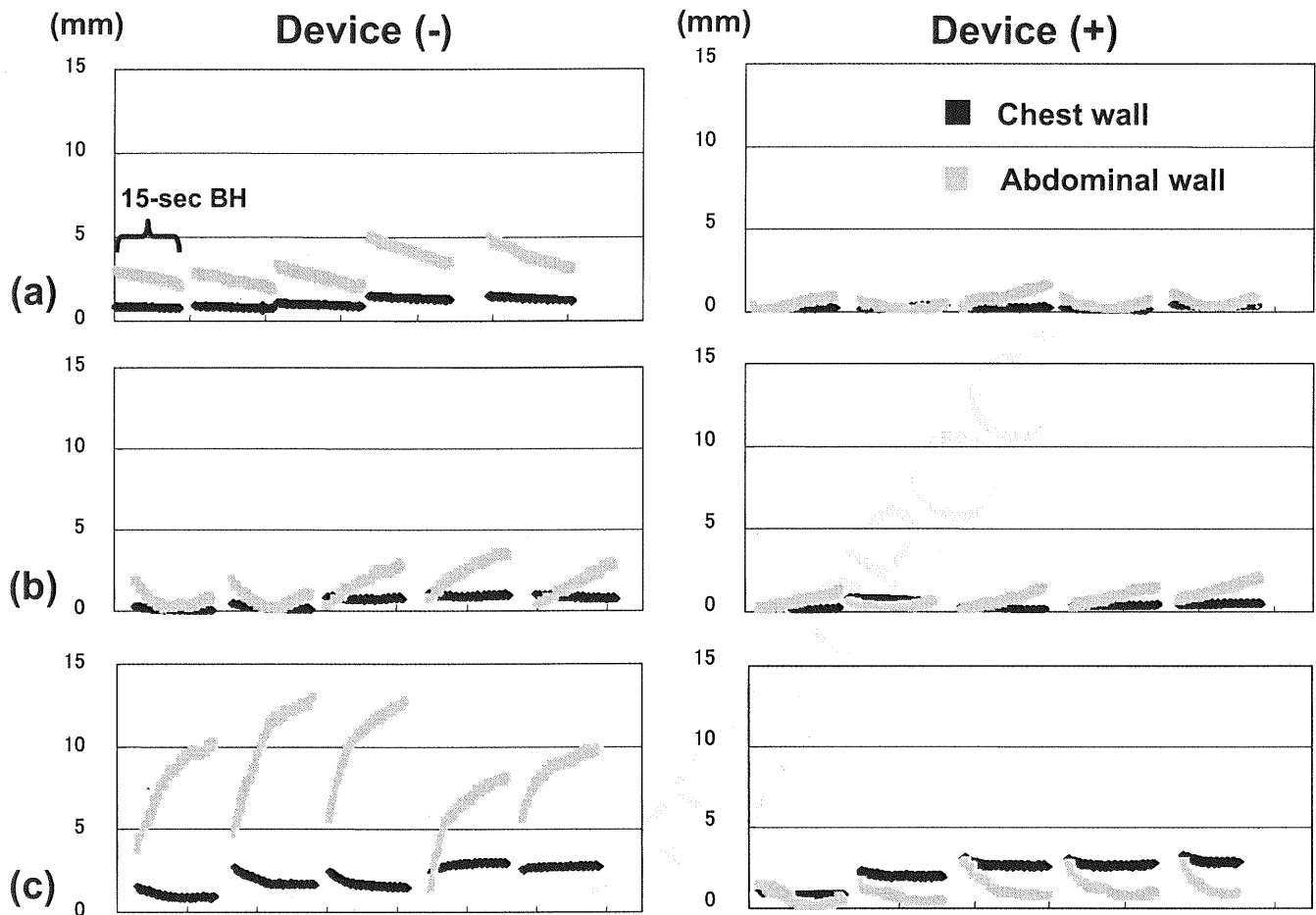


Fig. 4. The fluctuation in abdominal and chest wall positions during breath-holds. The vertical scale shows the movement of the fiducials (i.e., distance between the reference point and the wall position) during 5 repetitions of 15-s breath-hold in volunteer No. 4. The wall position was calculated only during the breath-holds. Between breath-holds, the volunteer breathed freely for 30–60 s. (a) Shallow expiration breath-hold, (b) shallow inspiration breath-hold, and (c) deep inspiration breath-hold.

Table 1. Summary of the results

| Device | SEBH | | SIBH | | DIBH | |
|---------------------|-----------|-----------|-----------|-----------|-----------|-----------|
| | (-) | (+) | (-) | (+) | (-) | (+) |
| Chest wall (mm) | | | | | | |
| Volunteer 1 | 1.2 ± 0.8 | 1.8 ± 0.5 | 0.7 ± 0.2 | 1.2 ± 0.3 | 2.4 ± 0.8 | 3.0 ± 1.8 |
| Volunteer 2 | 2.5 ± 1.8 | 0.3 ± 0.1 | 0.7 ± 0.4 | 0.5 ± 0.1 | 8.9 ± 7.0 | 2.6 ± 1.5 |
| Volunteer 3 | 1.1 ± 0.3 | 0.4 ± 0.2 | 0.6 ± 0.3 | 0.3 ± 0.1 | 2.0 ± 0.7 | 2.2 ± 0.8 |
| Volunteer 4 | 0.5 ± 0.3 | 1.2 ± 0.4 | 0.7 ± 0.5 | 2.0 ± 0.3 | 2.7 ± 0.6 | 2.4 ± 0.7 |
| Volunteer 5 | 0.7 ± 0.2 | 0.5 ± 0.2 | 0.6 ± 0.2 | 0.8 ± 0.6 | 2.2 ± 1.2 | 1.6 ± 0.7 |
| Mean | 1.2 ± 0.9 | 0.9 ± 0.3 | 0.6 ± 0.4 | 1.0 ± 0.4 | 3.7 ± 3.2 | 2.3 ± 1.2 |
| Abdominal wall (mm) | | | | | | |
| Volunteer 1 | 0.9 ± 0.6 | 2.8 ± 0.5 | 2.4 ± 1.2 | 1.8 ± 0.4 | 1.7 ± 1.1 | 3.0 ± 2.0 |
| Volunteer 2 | 2.6 ± 1.8 | 1.4 ± 0.3 | 4.9 ± 3.8 | 0.7 ± 0.3 | 7.0 ± 3.0 | 3.1 ± 1.7 |
| Volunteer 3 | 3.2 ± 0.9 | 0.8 ± 0.5 | 1.5 ± 1.0 | 0.6 ± 0.4 | 8.9 ± 2.3 | 1.0 ± 0.6 |
| Volunteer 4 | 2.1 ± 1.9 | 1.8 ± 0.6 | 2.3 ± 1.2 | 1.3 ± 0.5 | 7.0 ± 2.7 | 3.2 ± 0.6 |
| Volunteer 5 | 1.5 ± 0.7 | 0.7 ± 0.4 | 1.2 ± 0.7 | 0.9 ± 0.5 | 8.4 ± 2.2 | 2.5 ± 1.3 |
| Mean | 2.1 ± 1.3 | 1.5 ± 0.5 | 2.5 ± 1.9 | 1.1 ± 0.4 | 6.6 ± 2.4 | 2.6 ± 1.4 |

Abbreviations: SEBH = shallow expiration breath hold; SIBH = shallow inspiration breath hold; DIBH = deep inspiration breath hold.

1
2
3
4
5
6
7
8
9
10
11
12
13
14
15
16
17
18
19
20
21
22
23
24
25
26
27
28
29
30
31
32
33
34
35
36
37
38
39
40
41
42
43
44
45
46
47
48
49
50
51
52
53

phase than at the end-inspiration phase. Similar results were obtained in our study. However, with the aid of visual feedback, a reduction in the fluctuation of the wall position was obtained with both SEBH and SIBH. When a visual feedback system is available, radiotherapy may be performed at the end-inspiration phase because inhaling decreases lung density and excludes normal lung tissue from the high-dose region. However, this information may only be sufficient in healthy volunteers who are able to breathe with the abdomen. This technique should be evaluated in patients with limited breathing maneuvers.

For the gating technique with respiratory monitoring, the Varian Real Time Position Management (RPM) system (Varian Medical Systems, Palo Alto, CA) is frequently used (5, 16). This commercially available gating system includes an infrared camera mounted inside of the treatment room and connected to a desktop computer. To monitor respiration, plastic box with two passive reflective markers is placed on the anterior abdominal surface. The system tracks, displays, and records the vertical position of the marker. Although the exact position of the marker is identified, potential changes between fractions should be verified. In practice, the position of the tumor or an internal anatomic surrogate and gating thresholds are verified using fluoroscopy. Portal images are helpful to assess the performance of the monitoring system over the course of the treatment. After the operator has verified that the minimum and maximum vertical positions of the marker are stable and breathing is regular, the operator can send on-off control signals to a linear accelerator. Although our respiratory monitoring device can monitor the motion of the abdomen similarly, it cannot deliver a signal to the accelerator enabling beam delivery. Our system is simple and inexpensive. However, radiation should be turned on and off manually by the therapist.

In this series, the fluctuation of the wall position remained substantial during DIBH, even when the visual feedback technique was used. As reported by Remouchamps *et al.* (12), a moderate level of DIBH at 75% of the maximum inspiratory capacity or the assistance of BH using an active breathing control device may decrease such fluctuations in

wall position. One advantage of DIBH is that less tissue volume is irradiated than would be the case during normal respiration. Although DIBH is a promising technique, the wall motion observed during DIBH should still be monitored particularly carefully.

Unfortunately, all treatment techniques that deliver radiation during BHs are subject to patient compliance. Not all patients will tolerate treatment with this device equally during clinical use. Most lung cancer patients are elderly and may have respiratory lung dysfunctions. In addition, an important component of the visual feedback associated with this system is whether patients can successfully carry out abdominal breathing. A certain number of patients with compromised pulmonary function may not be able to maintain breath-hold with this device. However, if abdominal breathing is indeed realized, it is likely that the patient will benefit from the use of this simple and inexpensive device.

Another issue raised by this study involves ensuring the reproducibility of internal organ position between the different fractions (i.e., interfraction reliability). Although external monitors may show good correlation with the respiratory organs within a single session, the relationship between external monitor signals and internal organ positions may change between sessions. Ford *et al.* (22) evaluated gated localization radiographs from eight patients who received respiration-gated treatment during tidal breathing. The radiographs revealed an interfraction patient-averaged diaphragm variability of 2.8 ± 1.0 mm, although this variability was 6.9 ± 2.1 mm in the absence of gating. To decrease such interfraction variability, monitoring with film or portal imaging and repositioning before treatment is necessary.

We evaluated wall position using a machine vision system. This system can detect small changes in patient position with a resolution of less than 0.1 mm (21). It also enables the real-time monitoring of wall position during treatment. Therefore, the system may provide a means to detect respiratory motion. We are now beginning studies of the clinical use of the system for the treatment of lung and liver tumors.

REFERENCES

1. Ross CS, Hussey DH, Pennington EC, *et al.* Analysis of movement of intrathoracic neoplasms using ultrafast computerized tomography. *Int J Radiat Oncol Biol Phys* 1990;18:671-677.
2. Plathow C, Ley S, Fink C, *et al.* Analysis of intrathoracic tumor mobility during whole breathing cycle by dynamic MRI. *Int J Radiat Oncol Biol Phys* 2004;59:952-959.
3. Davies SC, Hill AL, Holmes RB, *et al.* Ultrasound quantitation of respiratory organ motion in the upper abdomen. *Br J Radiol* 1994;67:1096-1102.
4. Shimizu S, Shirato H, Ogura S, *et al.* Detection of lung tumor movement in real-time tumor-tracking radiotherapy. *Int J Radiat Oncol Biol Phys* 2001;51:304-310.
5. Mageras GS, Yorke E. Deep inspiration breath hold and respiratory gating strategies for reducing organ motion in radiation treatment. *Semin Radiat Oncol* 2004;14:65-75.
6. Onishi H, Kuriyama K, Komiyama T, *et al.* A new irradiation system for lung cancer combining linear accelerator, computed tomography, patient self-breath-holding, and patient-directed beam-control without respiratory monitoring devices. *Int J Radiat Oncol Biol Phys* 2003;56:14-20.
7. Minohara S, Kanai T, Endo M, *et al.* Respiratory gated irradiation system for heavy-ion radiotherapy. *Int J Radiat Oncol Biol Phys* 2000;47:1097-1103.
8. Tada T, Minakuchi K, Fujioka T, *et al.* Lung cancer: Intermittent irradiation synchronized with respiratory motion—results of a pilot study. *Radiology* 1998;207:779-783.
9. Hanley J, Debois MM, Mah D, *et al.* Deep inspiration breath-hold technique for lung tumors: The potential value of target immobilization and reduced lung density in dose escalation. *Int J Radiat Oncol Biol Phys* 1999;45:603-611.

10. Mah D, Hanley J, Rosenzweig KE, *et al.* Technical aspects of the deep inspiration breath-hold technique in the treatment of thoracic cancer. *Int J Radiat Oncol Biol Phys* 2000;48:1175–1185.
11. Rosenzweig KE, Hanley J, Mah D, *et al.* The deep inspiration breath-hold technique in the treatment of inoperable non-small-cell lung cancer. *Int J Radiat Oncol Biol Phys* 2000;48:81–87.
12. Remouchamps VM, Letts N, Vicini FA, *et al.* Initial clinical experience with moderate deep-inspiration breath hold using an active breathing control device in the treatment of patients with left-sided breast cancer using external beam radiation therapy. *Int J Radiat Oncol Biol Phys* 2003;56:704–775.
13. Balter JM, Lam KL, McGinn CJ, *et al.* Improvement of CT-based treatment-planning models of abdominal targets using static exhale imaging. *Int J Radiat Oncol Biol Phys* 1998;41:939–943.
14. Kimura T, Hirokawa Y, Murakami Y, *et al.* Reproducibility of organ position using voluntary breath-hold method with spirometer for extracranial stereotactic radiotherapy. *Int J Radiat Oncol Biol Phys* 2004;60:1307–1313.
15. Kini VR, Vedam SS, Keall PJ, *et al.* Patient training in respiratory-gated radiotherapy. *Med Dosim* 2003;28:7–11.
16. Nelson C, Starkschall G, Balter P, *et al.* Respiration-correlated treatment delivery using feedback-guided breath hold: A technical study. *Med Phys* 2005;32:175–181.
17. Carlson SK, Felmler JP, Bender CE, *et al.* Intermittent-mode CT fluoroscopy-guided biopsy of the lung or upper abdomen with breath-hold monitoring and feedback: System development and feasibility. *Radiology* 2003;229:906–912.
18. George R, Chung TD, Vedam SS, *et al.* Audio-visual biofeedback for respiratory-gated radiotherapy: Impact of audio instruction and audio-visual biofeedback on respiratory-gated radiotherapy. *Int J Radiat Oncol Biol Phys* 2006;65:924–933.
19. Plathow C, Zimmermann H, Fink C, *et al.* Influence of different breathing maneuvers on internal and external organ motion: Use of fiducial markers in dynamic MRI. *Int J Radiat Oncol Biol Phys*. 2005;62:238–245.
20. Gierra DP, Brewer J, Sharp GC, *et al.* The correlation between internal and external markers for abdominal tumors: Implications for respiratory gating. *Int J Radiat Oncol Biol Phys*. 2005;61:1551–1558.
21. Yoshitake T, Nakamura K, Shioyama Y, *et al.* A machine vision system with CCD cameras for patient positioning in radiotherapy: A preliminary report. *Fukuoka Igaku Zasshi* 2005;96:399–405.
22. Ford EC, Mageras GS, Yorke E, *et al.* Evaluation of respiratory movement during gated radiotherapy using film and electronic portal imaging. *Int J Radiat Oncol Biol Phys* 2002;52:522–531.

62
63
64
65
66
67
68
69
70
71
72
73
74
75
76
77
78
79
80
81
82
83
84
85
86
87
88
89
90
91
92
93
94
95
96
97
98
99
100
101
102
103
104
105
106
107
108
109
110
111
112
113
114